

1
2
3
4
5
6 1 A stochastic movement model reproduces patterns of site
7
8
9 2 fidelity and long-distance dispersal in a population of
10
11
12 3 Fowler's Toads (*Anaxyrus fowleri*)
13
14

15 4
16
17 5 Philippe Marchand*, National Socio-Environmental Synthesis Center (SESYNC), Annapolis,
18
19 6 MD 21401, United States.

20
21 7 Morgan Boenke, Department of Biology, McGill University, Montreal, Quebec H3A 1B1,
22
23 8 Canada.

24
25 9 David M. Green, Redpath Museum, McGill University, Montreal, Quebec H3A 0C4, Canada.
26
27

28 10

29
30 11 * Corresponding author: marchand.philippe@gmail.com. ORCID: 0000-0001-6717-0475.
31

32 12

33
34 13
35
36
37
38
39
40
41
42
43
44
45
46
47
48
49
50
51
52
53
54
55
56

57
58
59
60
61
62
63
64
65
66
67
68
69
70
71
72
73
74
75
76
77
78
79
80
81
82
83
84
85
86
87
88
89
90
91
92
93
94
95
96
97
98
99
100
101
102
103
104
105
106
107
108
109
110
111
112

14 **Abstract**

15 Although amphibians typically exhibit high site fidelity and low dispersal, they do
16 undertake rare, long-distance movements. The factors influencing these events remain poorly
17 understood, partly because amphibian spring movements tend to radiate from breeding sites and
18 the animals are often difficult to locate at other times of the year. In this study, we investigate
19 whether these movement patterns can be reproduced by a parsimonious model where foraging
20 steps follow a heavy-tailed, Lévy alpha-stable distribution and individuals may either return to a
21 previous refuge site or establish a new one. We consider three versions of the return behaviour:
22 (1) a distance-independent probability of return to any previous refuge; (2) constant probability
23 of return to the nearest refuge; or (3) a distance-dependent probability of return to each refuge.
24 Using approximate Bayesian computation, we fit each version of the model to radiotracking data
25 from a population of Fowler’s Toads, which inhabits a linear sand dune habitat on the north shore
26 of Lake Erie in Ontario, Canada. Only the model with distance-independent, random returns
27 provides a good fit of the inter-refuge distance distribution and the number of refuges visited per
28 toad. Our results suggest that while toads occasionally forage over long distances, the
29 establishment of new refuges is not driven by the minimization of energy expenditure.

30
31 **Keywords:** amphibian; animal movement; approximate Bayesian computation; foraging; Lévy
32 walk; radiotracking

33

113
114
115
116
117 **34 1. Introduction**
118

119
120 35 The movements that individual animals undertake to go from place to place are
121
122 36 fundamental to virtually every aspect of animal ecology and behaviour. How small movements
123
124 37 of animals at daily or hourly scales result in such larger phenomena as home-ranges, dispersal
125
126 38 and migrations at seasonal, annual or life-time scales, however, remains a difficult problem to
127
128 39 understand. It has commonly been observed that a high-frequency of short-distance movements
129
130 40 combined with rare, long-distance movement events results in a movement step size distribution
131
132 41 that is strongly leptokurtic, with a sharper peak and longer tails than expected of a normal
133
134 42 distribution, and possibly heavy-tailed, i.e. with the long-distance probability tail extending past
135
136 43 that of an exponential distribution (e.g., Cecala et al., 2009; Gomez and Zamora, 1999; Morales,
137
138 44 2002; Paradis et al., 1998; Skalski and Gilliam, 2000). Such heavy-tailed distributions in animal
139
140 45 movement may be consistent with the Lévy flight foraging hypothesis (Viswanathan et al.,
141
142 46 1999), according to which optimal search patterns follow a power-law distribution of step sizes,
143
144 47 with the frequency of steps proportional to some inverse power of their length. However, tests of
145
146 48 this hypothesis have been the subject of numerous statistical challenges (Edwards, 2011).
147
148

149
150 49 In actuality, animal movement is not scale-free and must be constrained by biological
151
152 50 limits, so that the power-law distribution can only hold within a certain range of step sizes
153
154 51 (Benhamou, 2007). Over the longer time scales that encompass multiple individual movements,
155
156 52 such as may occur during foraging or dispersal behaviours, movement distances may also depend
157
158 53 on the animal's memory and "cognitive map" of the environment, features that are poorly
159
160 54 represented in movement models based on independent steps (Gautestad and Myrsetrud, 2013).
161
162 55 More complex models that can accommodate both specific movement rules and memory effects
163
164
165
166
167
168

169
170
171
172
173 56 may be required, but their outcomes may not be expressible in terms of analytical likelihood
174
175
176 57 functions.

177
178 58 Although the absence of a likelihood function previously precluded formal statistical
179
180 59 analysis, computational and statistical advances in the last 20 years have made it possible to
181
182 60 derive inferences from simulation-based models (Hartig et al., 2011). Approximate Bayesian
183
184 61 computation (ABC) is a simulation-based inference method originally developed in the field of
185
186 62 population genetics, wherein the large number of possible genetic histories and intermediate
187
188 63 states leading to a given outcome make explicit likelihood calculations intractable (Beaumont et
189
190 64 al., 2002). Since analogous challenges, i.e. path dependence and a large number of unobserved
191
192 65 intermediate states, are also encountered in the study of animal movement, ABC provides a
193
194 66 flexible mean to test foraging and dispersal behaviour models with empirical data (Marchand et
195
196 67 al., 2015).

197
198
199 68 Anuran amphibians, although they have generally been considered poor dispersers
200
201 69 relative to larger, more vagile terrestrial vertebrates, can be valuable subjects for testing models
202
203 70 of animal movement. Individuals may show a high level of site fidelity yet mark-recapture
204
205 71 studies have also shown that anurans will undertake relatively rare long-distance movements of
206
207 72 up to a few km in a matter of days, or as far as 35km over the course of a season (Smith and
208
209 73 Green, 2005, 2006). Whether site fidelity is advantageous should depend on the tradeoff
210
211 74 between the benefit of a known location relative to the cost of returning to that location (Wells,
212
213 75 2007). As many amphibian species make use of refuge sites as part of their daily activity cycles,
214
215 76 this makes discretizing movement simpler as time periods between movement steps are more or
216
217 77 less standardized and biologically meaningful. Nevertheless, locating individual anurans outside
218
219
220
221
222
223
224

225
226
227
228
229 78 of the breeding season can be difficult with many species as they tend to be mostly nocturnal
230
231 79 foragers that hide during the daytime. Moreover, the small size of most species precludes the use
232
233 80 of GPS satellite telemetry methods that can provide long-term, high-resolution movement time-
234
235 81 series for larger terrestrial animals (Wikelski et al., 2007). Both of these difficulties can be
236
237 82 overcome, however, with the appropriate model species.

240 83 In this study, we develop a parsimonious model that describes both site fidelity and long-
241
242 84 distance movements, and apply this model to the movements of Fowler's Toads (*Anaxyrus*
243
244 85 *fowleri*) in a population inhabiting a linear sand dune habitat on the north shore of Lake Erie in
245
246 86 Ontario, Canada. In this environment, adult Fowler's Toads are readily locatable as they forage
247
248 87 on the beaches at night (Greenberg and Green, 2013). Previous capture-mark-recapture data
249
250 88 (Smith and Green 2005, 2006) have established and quantified the heavy-tailed movement
251
252 89 distribution curve of these toads. The toads can also be fitted with small radio-transmitters
253
254 90 (Boenke, 2011), which allow them to be tracked to their daytime hiding places in the sand dunes
255
256 91 fronting the beaches. Based on this radiotracking data, we use ABC to estimate the parameters of
257
258 92 the movement model, including the scale and shape of a Lévy-stable distribution of movement
259
260 93 steps and the probability of returning to a known refuge rather than establishing a new one.

263 94 To assess the importance of energy constraints on movement, we compare the relative fit
264
265 95 of three versions of the return step: (1) toads return to a randomly selected previous refuge,
266
267 96 independent of distance; (2) they return to the nearest refuge from their current location; or (3)
268
269 97 the probability of return to any previous refuge is a decreasing function of the distance to that
270
271 98 refuge. We hypothesize that either of the last two models would provide a better fit if minimizing
272
273 99 energy expenditure were the primary factor determining refuge choice.
274
275
276
277
278
279
280

281
282
283
284
285
286
287
288
289
290
291
292
293
294
295
296
297
298
299
300
301
302
303
304
305
306
307
308
309
310
311
312
313
314
315
316
317
318
319
320
321
322
323
324
325
326
327
328
329
330
331
332
333
334
335
336

100
101
102
103
104
105
106
107
108
109
110
111
112
113
114
115
116
117
118
119
120
121

2. Methods

2.1. Study site and population

We studied the movement ecology of Fowler’s Toads at Long Point in Ontario, Canada, along the beaches of Long Point Provincial Park and the Long Point National Wildlife Area Thoroughfare Point Unit (UTM zone 17 N: 550700 – 553000 Easting, 4713615 – 4714200 Northing; NAD 83 Datum). Although the dune ecosystems along the north shore of Lake Erie are highly dynamic (Gelinas and Quigley, 1973; Stenson, 1993), human disturbance at this site is minimal and movement by toads not constrained either by lack of suitable habitat or by lack of connectivity between habitat patches (Smith and Green, 2005, 2006). The toads generally take refuge in the sand dunes fronting the beach during the day and emerge to forage for invertebrate prey along the lakeshore at night.

2.2. Stochastic movement model

To reflect both the high rate of apparent site fidelity and the heavy-tailed distribution of dispersal steps present in the previous mark-recapture data (Smith and Green, 2006), we used a variant of the multiscaled random walk (MRW) model proposed by Gautestad and Myserud (2005). The MRW is based on a power-law step length distribution, but differs from a classic Lévy flight by allowing a certain frequency of return steps, wherein the individual revisits a location chosen at random from previous points in the walk. As each successive visit to a location increases its effective weight for future return steps, the MRW model allows home range patterns to emerge without the need to specify an *ad hoc* homing process.

337
338
339
340
341 122 In our model, we assumed that return steps only occurred at the end of the nighttime
342
343 123 foraging path, when the toad is at a position Δx_n away from the previous day's refuge site. At this
344
345 124 point, the toad either takes refuge at its current position or returns to a known refuge site.

347 125 2.2.1. Return steps

349 126 Our three model versions differ in how they describe the return behaviour:

350 127 Model 1 (random return): The probability of return is constant ($p_{ret} = p_0$), and the toad selects a
351
352 128 refuge at random from all the previous days' refuges. As in Gautestad and Myrsetrud's model,
353
354 129 multiple visits to a refuge increase its "weight" for future return steps.

355 130 Model 2 (nearest return): The probability of return is constant ($p_{ret} = p_0$), but the toad always
356
357 131 returns to the nearest refuge.

358 132 Model 3 (distance-based return probability): The probability of returning to a given site decays
359
360 133 exponentially with the distance d_i to that refuge:

$$361 134 p_{ret(i)} = p_0 e^{-\frac{d_i}{d_0}}, \quad (1)$$

362 135 where d_0 is a characteristic distance to be estimated along with p_0 . The probability of not
363
364 136 returning to any previous site is the product of the complements of the $p_{ret(i)}$:

$$365 137 1 - p_{ret} = \prod (1 - p_{ret(i)}) , \quad (2)$$

366 138 where R is the number of *distinct* previous refuges.

367 139 In the case of a return event, the probability of each refuge being chosen is given by:

$$370 140 P(\text{return at } i | \text{return}) = \frac{p_{ret(i)}}{\sum p_{ret(i)}} . \quad (3)$$

371 141 With an additional parameter, the third model allowed us to consider intermediate cases
372
373 142 of distance-dependence. As the characteristic distance d_0 decreases, it becomes increasingly

337
338
339
340
341
342
343
344
345
346
347
348
349
350
351
352
353
354
355
356
357
358
359
360
361
362
363
364
365
366
367
368
369
370
371
372
373
374
375
376
377
378
379
380
381
382
383
384
385
386
387
388
389
390
391
392

393
394
395
396
397 143 likely that the toad will choose the nearest refuge; yet the outcome differs from that of model 2,
398
399 144 since the probability of return is not constant but decreases with distance. In the limit where d_0 is
400
401 145 very large, $p_{\text{ret}(i)} = p_0$ and all previous sites have the same probability of return. Contrary to model
402
403 146 1, however, the probability of returning to any site is not constant but increases with R (as a
404
405 147 consequence of Eq. 2). Moreover, since model 3 considers distinct refuge sites, multiple visits to
406
407 148 the same refuge do not increase its probability weight.
408
409
410
411

412 150 2.2.2. Overnight displacement

413
414 151 The net overnight displacement, Δx_n , in the model followed a symmetric, zero-centered
415
416 152 stable (a.k.a. Lévy alpha-stable) distribution, $S(\alpha, \gamma)$, with stability parameter α ($0 < \alpha \leq 2$) and
417
418 153 scale parameter $\gamma > 0$. With $\alpha = 2$, the stable distribution reduces to a normal law, whereas
419
420 154 decreasing values of α produced increasingly leptokurtic (i.e. heavy-tailed) distributions,
421
422 155 including the Cauchy distribution ($\alpha = 1$) as a special case (Uchaikin and Zolotarev, 1999). For α
423
424 156 < 2 , the tails of the probability density followed a power law decay with exponent $-(1 + \alpha)$.
425
426

427 157 Although there is no closed form of the stable probability density for arbitrary α , random
428
429 158 draws from $S(\alpha, \gamma)$ can be generated by the CMS algorithm (Chambers *et al.* 1976):
430
431

$$432 \quad 159 \quad S = \gamma \frac{\sin \alpha U}{(\cos U)^{\frac{1}{\alpha}}} \left[\frac{\cos((1 - \alpha)U)}{W} \right]^{\frac{1 - \alpha}{\alpha}}, \quad (4)$$

433
434
435
436 160 where U is a uniformly distributed angle in $(-\pi, \pi)$ and W has a standard exponential
437
438 161 distribution.
439

440
441 162 A key property of the stable distribution is that the sum of stable random variables is also
442
443 163 stable; in particular, the sum of N independent variables distributed as $S(\alpha, \gamma)$ is stable with the
444
445
446
447
448

449
450
451
452
453 164 same stability parameter α and a scale $\gamma_N = N^{1/\alpha}\gamma$. Furthermore, the generalized central limit
454
455 165 theorem of Gnedenko and Kolmogorov (1954) shows that the sum of independent variables
456
457
458 166 following a common distribution with asymptotic power-law tail converges to a stable
459
460 167 distribution.

461
462 168 Given these properties, our assumption that Δx_n has a stable distribution was robust to
463
464 169 differences in the small-scale foraging behaviour. For example, while foraging steps are probably
465
466 170 correlated on a short-term scale, as long as there is some intermediate time scale where
467
468 171 successive displacements can be modelled as independent and following a heavy-tailed (power-
469
470 172 law) distribution, the stable distribution will be a reasonable approximation of net displacement.
471

472 173

474 174 ***2.3. Model fitting with approximate Bayesian computation***

475
476 175 We fitted our model by approximate Bayesian computation (ABC) using the ABC-
477
478 176 rejection algorithm, as implemented in the ‘abc’ package (Csilléry et al., 2012) in R (R Core
479
480 177 Team, 2016). Consider a simulation model that takes an input parameter vector θ and outputs a
481
482 178 vector of summary statistics (S) calculated from the simulation outcome. Given a set of θ
483
484 179 vectors, drawn from the parameters’ prior distributions, and a corresponding set of simulation
485
486 180 outputs $S(\theta)$, ABC-rejection simply selects a subset of θ for which the output statistics are close
487
488 181 to those of the observed data D , i.e. where $d[S(\theta), S(D)] < \varepsilon$ for a chosen distance function d and
489
490 182 tolerance level ε . The selected subset approximates the joint posterior distribution of θ . The
491
492 183 approximation accuracy can be further improved by fitting a local-linear regression model of θ
493
494 184 vs. $S(\theta)$ and using that empirical model to correct each θ towards the value it would have at $S(D)$
495
496 185 (Beaumont et al., 2002).
497
498
499
500
501
502
503
504

505
506
507
508
509 186 The ABC-rejection algorithm can be naturally extended to the problem of model selection
510
511 187 by treating the choice of model as a discrete parameter (Toni et al., 2009). If the number of
512
513 188 simulations run under each model is proportional to its prior probability, then the representation
514
515 189 of a model among the simulations retained following the rejection step is an estimate of its
516
517 190 posterior probability. As in the parameter estimation case, the approximation can be improved by
518
519 191 fitting a regression of the discrete model probabilities, i.e. a multinomial logistic regression, as a
520
521 192 function of the summary statistics in the vicinity of the observed statistics (Beaumont, 2008).
522
523

524 193 The main drawback of ABC-rejection is the high number of simulations necessary to get
525
526 194 a sufficient number of results in the vicinity of the data. Alternative ABC algorithms use Markov
527
528 195 chain Monte Carlo or sequential Monte Carlo (a.k.a. particle filter) methods to gradually
529
530 196 concentrate the sampling effort in the areas of high-agreement between simulated and observed
531
532 197 statistics (Marjoram et al., 2003; Sisson et al., 2007). Yet, ABC-rejection has the advantage of
533
534 198 decoupling the simulation and estimation steps, which allows the entire set of simulations to be
535
536 199 run ahead of time and, possibly, in parallel on a high-performance computing cluster. Multiple
537
538 200 estimations can then be performed from this set of simulation outputs, which is especially helpful
539
540 201 when performing cross-validation.
541
542

543 202

544 203 *2.3.1. Prior distributions and summary statistics*

545
546 204 Our results were based on 10,000 simulations of each version of the stochastic model. For
547
548 205 each simulation, we drew parameters from the following uniform prior distributions: $\alpha \sim U(1, 2)$,
549
550 206 $\gamma \sim U(10m, 100m)$, $p_0 \sim U(0, 1)$ and (for model 3 only) $d_0 \sim U(20m, 2000m)$. To match the size
551
552 207 and structure of the observed dataset, we simulated the movement of 66 toads over 63 days, then
553
554
555
556
557
558
559
560

561
562
563
564
565
566
567
568
569
570
571
572
573
574
575
576
577
578
579
580
581
582
583
584
585
586
587
588
589
590
591
592
593
594
595
596
597
598
599
600
601
602
603
604
605
606
607
608
609
610
611
612
613
614
615
616

208 subset the results to keep only the (Toad, Day) observation points present in the data. For each of
209 four different time lags (1, 2, 4 and 8 days), we calculated three statistics over all pairs of points
210 with the same toad and the corresponding time lag: (1) the frequency of returns (defined as $|\Delta x| <$
211 10m), as well as (2) the mean and (3) standard deviation of $\log(\Delta x)^2$ for non-returns, over all
212 pairs of points with the same toad and corresponding time lag. We chose these 12 summary
213 statistics as well as the 10m distance threshold to capture the key characteristics of the empirical
214 distribution of relocation distances at multiple time scales (see section 3.1 and Fig. 1). We used
215 the Euclidean distance (sum of squared differences) to compare this vector of summary statistics
216 to the corresponding statistics of the radiotracking data.

217

218 2.3.2. Cross-validation

219 We used the ‘abc’ package’s cross-validation feature to verify the identifiability of our
220 model, i.e. determining whether the size of the dataset and the chosen summary statistics are
221 sufficient to estimate the parameters of interest for each model version, and distinguish the
222 outcome of the alternate model versions. We also used cross-validation to choose an optimal
223 tolerance rate, which is the fraction of best-fitting simulations to keep for estimating the posterior
224 distribution.

225 For the parameter estimation problem, cross-validation was performed separately for
226 each model version. Taking one of the simulation results as the “data”, we applied ABC to
227 estimate the true parameters of that simulation based on the remainder of the simulation results.
228 We repeated this process for 100 sampled simulation results and four different tolerance rates
229 (0.5%, 1%, 5% and 10%). The cross-validation accuracy was quantified using the relative

617
618
619
620
621 230 estimation error, defined as the mean square difference between estimated and true parameter
622
623
624 231 values divided by the variance of the true values over the 100 sampled simulations.

625
626 232 For the model selection problem, cross-validation consisted in taking one simulation
627
628 233 output as the data and applying ABC to the remaining 29,999 simulation results (combined from
629
630 234 all three models) to estimate the posterior probabilities of each model version. We repeated this
631
632 235 process for 100 sampled simulations per model version, using the same tolerance rates as above.
633
634 236 Model selection accuracy is quantified by the misclassification rate: the fraction of cases where
635
636 237 the model version with the highest posterior probability differed from the true model.
637

638
238

639 239 *2.3.3. Parameter estimates and model selection*

640
641
642
643 240 We estimated the posterior distribution of each parameter via ABC-rejection, using the
644
645 241 tolerance rate selected by cross-validation and applying the local-linear regression correction of
646
647 242 Beaumont et al. (2002). For the regression correction, we applied a logit transformation to the
648
649 243 stability parameter (α) to keep the inferred values within the (1, 2) bounds, and a log
650
651 244 transformation to d_0 to constrain its range to positive values. Parameters were estimated
652
653 245 separately for the three versions of the model.

654
655 246 To compare the fit of the different model versions, we first estimated the posterior
656
657 247 probabilities of the three models by ABC-rejection, followed by multinomial logistic regression
658
659 248 of model probabilities in the vicinity of the observed summary statistics (Beaumont 2008). We
660
661 249 then verified that simulation outputs from the fitted version of each model (with parameters
662
663
664 250 drawn from their posterior distribution) could reproduce the observed summary statistics.
665
666
667
668
669
670
671
672

673
674
675
676
677
678
679
680
681
682
683
684
685
686
687
688
689
690
691
692
693
694
695
696
697
698
699
700
701
702
703
704
705
706
707
708
709
710
711
712
713
714
715
716
717
718
719
720
721
722
723
724
725
726
727
728

251 As an additional posterior predictive check, we compared the number of distinct refuge
252 sites in the simulated and observed datasets. In practice, we defined this quantity as the number
253 of clusters obtained at a distance threshold of 10m, when performing hierarchical clustering of
254 the point locations using the complete-linkage method ('hclust' function in R). The complete-
255 linkage criterion ensures that each pair of points in the cluster is separated by no more than the
256 specified distance threshold.

257

258 **2.4. Radiotracking data**

259 We collected radiotracking data on Fowler's Toads at our study site during mid-June to
260 late August of 2009 and 2010 (Boenke, 2011). Toads were captured opportunistically while they
261 were foraging on the beach, and outfitted with either Holohil BD-2 (in 2009) or BD-2N (in 2010)
262 radiotransmitters, which were attached to the toad via a filament covered in plastic tubing
263 (following Bartelt and Peterson, 2000). The total weight of the transmitter and harness (ca. 2 g)
264 constituted ~5% of the typical adult toad weight, and in no case exceeded 10% of the
265 individual's weight, as recommended by Rowley and Alford (2007). Toads were tracked with an
266 HR2600 Osprey Receiver (H.A.B.I.T. Research, Victoria, BC, Canada) and Yagi 3-element
267 antenna. Upon finding each toad, its position was recorded with a Magellan Mobile Mapper 6
268 GPS unit (Magellan Navigation, Inc., Santa Clara, CA, USA). The location of each tracked toad
269 was recorded at least once per night (active foraging) and once per day (resting in refuge) but we
270 only used the daytime locations in the present study. The number of consecutive days in a
271 tracking bout varied by toad, as some individuals shed their transmitter, or else it had to be
272 removed to alleviate skin irritation. Since individuals were identified by toe clipping or

729
730
731
732
733 273 distinctive marks from digital photographs, toads that lost their transmitter could sometimes be
734
735 274 retrieved, allowing multiple tracking bouts per toad (Boenke, 2011). All procedures with animals
736
737
738 275 were conducted under McGill University Animal Use Protocol No. 4569.

739
740 276 The position of toads' daytime refuges relative to the shore is governed by tradeoffs between
741
742 277 wave avoidance, predator avoidance, elevation and proximity to water (Boenke, 2011). In
743
744 278 contrast, movement along the shoreline is unconstrained, meaning that dispersal occurs mostly
745
746 279 along a single dimension. For this reason, we projected all refuge locations on a single axis,
747
748 280 obtained by linear regression of the two-dimensional coordinates, and only modeled this one-
749
750 281 dimensional component of toad movement.

752
753 282

754 283 *2.5. Source code and data access*

755
756
757 284 The dataset used for this study and the R code for all simulation and analyses can be
758
759 285 downloaded from GitHub: <http://github.com/pmarchand1/fowlers-toad-move/>.

760
761 286

762 763 287 **3. Results**

764 765 288 *3.1. Empirical distribution of relocation distances*

766
767 289 The radio-tracking dataset included 66 toads, with between 2 and 30 daytime points
768
769 290 recorded, for a mean of 12 locations per toad per season.

770
771
772 291 When shown on a logarithmic scale (Fig. 1), the distribution of distances between
773
774 292 daytime refuges of a toad was characterized by a symmetric peak combined with an inflated
775
776 293 number of low-distance events. Given the GPS margin of error of 3 – 5m per point, distances of
777
778 294 less than 10m could not be measured reliably (Boenke, 2011). Therefore, the excess probability
779
780
781
782
783
784

785
786
787
788
789 295 in that part of the distribution would be consistent with toads returning to previous sites. In
790
791 296 contrast with the expectations of a random walk model, where the whole distribution would shift
792
793 297 to larger distances as the time step increases, the peak of relocation distances varied little
794
795 298 between time lags of 1 to 8 days. Instead, longer time lags increased the total probability on the
796
797 299 high end of the distribution as the fraction of short-distance (or return) events decreased.
798
799
800
801

802 301 ***3.2. Approximate Bayesian computation***

803 302 *3.2.1 Cross-validation*

804 303 With the exception of d_0 in model 3 (see below), the cross-validation results (Table S1 in
805
806 304 the supplementary data) showed a good agreement between the true values of the parameters and
807
808 305 their posterior median estimated via ABC. Overall, the relative estimation error was minimized
809
810 306 with a 5% tolerance level; the supplementary Fig. S1 shows how the estimated and true values
811
812 307 compare across all parameters at that tolerance level. For all three model versions, the relative
813
814 308 error was higher for α (10% to 14%) than for γ (around 7%) or p_0 (1% to 5%). Since α
815
816 309 determines the power-law tail of the stable distribution, its value is sensitive to rare, long-
817
818 310 distance events, which could explain the higher estimation variance. The characteristic distance
819
820 311 d_0 had the highest estimation error, at over 60% of the prior range. Therefore, this parameter
821
822 312 might only be identifiable with a larger dataset.
823
824
825
826

827 313 The ABC model selection algorithm could discriminate well between Model 2 and either
828
829 314 other version. However, 35% of the Model 1 runs were misidentified as Model 3 and 23% of
830
831 315 Model 3 runs were misidentified as Model 1 (Table 1). This is consistent with the behaviour of
832
833 316 Model 3 approaching random returns in the limit of high d_0 ; while there are still differences
834
835
836
837
838
839
840

841
842
843
844
845 317 between the two models in that limit, they might not be detectable with the chosen summary
846
847
848 318 statistics.

849 319 *3.2.2. Parameter estimation*

850
851
852 320 The posterior median and 95% Bayesian credible interval for all parameter estimates are
853
854 321 shown in Table 2. The estimates of the stable distribution parameters were similar for Model 1 (α
855
856 322 = 1.7, $\gamma = 34$ m) and Model 3 ($\alpha = 1.65$, $\gamma = 32$ m), whereas both values were higher for Model 2
857
858 323 ($\alpha = 1.83$, $\gamma = 46$ m).

860
861 324 The estimated values of α suggest a power-law tail with an exponent between -2.6 and
862
863 325 -2.8 . The estimates of α could be biased upwards, however, since long-distance dispersal events
864
865 326 are more likely to take toads outside of the tracking range. That is, the power-law tail could
866
867 327 extend further than inferred from the data.

869 328 As expected based on the poor cross-validation results, the estimate of d_0 in model 3 has a
870
871 329 very wide credible interval (220 to 1697 m). In comparison, the largest distance between any two
872
873 330 observations of the same toad in the dataset was 1198 m, and only 4 out of 66 toads visited
874
875 331 locations more than 350 m apart. Most of the posterior distribution thus lies in the high d_0 range
876
877 332 where refuge choice is not primarily constrained by distance. Note that the estimates of p_0 in
878
879 333 Model 3 (0.43) and Model 1 (0.60) are not directly comparable even in the distance-independent
880
881 334 case, since the actual probability of return in Model 3 increases with the number of visited
882
883 335 refuges (see section 2.2).

884
885 336 We verified that our posterior parameter estimates did not significantly change when
886
887
888 337 performing additional simulations beyond the current 10,000 per model version (Fig. S2 in the
889
890 338 supplementary data).
891
892
893
894
895
896

897
898
899
900
901
902
903
904
905
906
907
908
909
910
911
912
913
914
915
916
917
918
919
920
921
922
923
924
925
926
927
928
929
930
931
932
933
934
935
936
937
938
939
940
941
942
943
944
945
946
947
948
949
950
951
952

339 *3.2.3. Model selection*

340 The ABC model selection process resulted in posterior probabilities of 15% for Model 1
341 (random return), 0% for Model 2 (nearest return) and 85% for Model 3 (distance-dependent
342 return probability). Given the high probability of misclassification between Model 1 and 3 (Table
343 1) and the difference in complexity between the two models (3 versus 4 adjustable parameters),
344 this result alone does not provide strong evidence of a better fit for Model 3.

345 The comparison of observed and simulated summary statistics from the three models,
346 with simulation parameters drawn from their respective posterior distribution, shows that Model
347 2 is too dispersive. That is, the mean log distance increases – and the probability of return
348 decreases – too rapidly with greater time lags. In contrast, the range of simulated results from
349 Models 1 and 3 is consistent with the observed statistics at all time lags (Fig. 2).

350 Finally, we computed the number of distinct refuge sites, defined in section 2.3 as
351 clusters of points with diameter less than 10m, for each toad in both the empirical data and the
352 output of each simulation model (with parameters drawn from their posterior distribution). This
353 quantity is strongly dependent on the number of observations by individual; our results show that
354 this relationship can be well approximated by a linear regression on a log-log plot (Fig. 3). Note
355 that the simulation results show less variance as they represent the average of 500 simulated
356 paths by toad. This number of refuges statistic, which wasn't directly used in fitting the
357 parameters of each model, shows a better fit for Model 1: the 95% confidence intervals of the
358 regression lines for observed and simulated points overlap. Model 3, in contrast, results in too
359 few distinct refuges for toads with many observations. This may be due to the functional form of

953
954
955
956
957
958
959
960
961
962
963
964
965
966
967
968
969
970
971
972
973
974
975
976
977
978
979
980
981
982
983
984
985
986
987
988
989
990
991
992
993
994
995
996
997
998
999
1000
1001
1002
1003
1004
1005
1006
1007
1008

360 the probability of return in this model (Eq. 2), which increases with the number of distinct
361 refuges already visited.

362

363 **4. Discussion**

364 In the analysis above, we showed that a parsimonious model of foraging behaviour (our
365 Model 1) successfully reproduced the main patterns of refuge site fidelity and relocation among a
366 population of Fowler's Toads. The model assumed that the net displacements of toads during
367 nighttime foraging follows a heavy-tailed, Lévy-stable distribution, and that toads may either
368 take refuge at the end of their foraging path, or return to a random refuge among those previously
369 visited.

370 The assumption that toads returning to a previous refuge choose one at random may seem
371 unrealistic. Yet it fit the data better than two alternative models we tested, where the probability
372 of return and/or the choice of refuge were distance-dependent. It might be that movement cost is
373 only one of many factors determining refuge selection, along with slope, elevation and
374 vegetation cover of potential refuge sites (Boenke, 2011). Without knowing the spatial structure
375 of these microhabitat variables along the beach length, it is difficult to determine how they could
376 affect the movement statistics. Even if additional environmental data were available, the size of
377 the tracking dataset (individuals and locations per individual) would also set a limit to the
378 complexity of verifiable models: the very diffuse posterior distribution for the characteristic
379 distance d_0 in model 3 provides a good example of this problem.

380 Even for this simple model, this study illustrates the power and flexibility of approximate
381 Bayesian computation for the calibration and testing of mechanistic movement models from field

1009
1010
1011
1012
1013 382 data. In particular, ABC doesn't require the stochastic process of interest to have a known
1014
1015 383 analytical likelihood, and it can easily accommodate gaps in observations (by subsetting the
1016
1017
1018 384 simulated data) as well as sources of error and censoring. In this study, we took into account the
1019
1020 385 unreliability of GPS measurements at short distances, and if we had an independent measure of
1021
1022 386 long-distance censoring, that effect could have been included as well.

1023
1024 387 Our results indicate that long-term movement patterns, such as dispersal, may be
1025
1026 388 profoundly affected by small-scale micro-habitat choices and day-to-day movement. Sand dunes
1027
1028 389 and beaches are highly dynamic environments that are strongly affected by both weather
1029
1030 390 conditions and waves. The large temporal variation in habitat quality, combined with a relatively
1031
1032 391 lower spatial variability in the direction parallel to the shore, matches conditions that have been
1033
1034 392 found to favor heavy-tailed movement patterns (Lowe, 2009). Temporal habitat variability can
1035
1036 393 also contribute to the decrease in the probability of return with larger time steps, as preferable
1037
1038 394 refuge locations shift during the season.

1039
1040 395 This stochastic movement model, calibrated through individual-level tracking data,
1041
1042 396 provides a measure of home range size that is robust to changes in the scale or number of
1043
1044 397 observations. We note that while the number of refuge sites utilized by a toad increases with the
1045
1046 398 number of observation days, the median relocation distance (the peak on the log scale of Fig. 1)
1047
1048 399 varies little with time. This suggests that most toads' movement remains within that spatial
1049
1050 400 range. Conversely, the probability of rare, long-distance dispersal events predicted by the model
1051
1052 401 can serve to estimate the level of connectivity between toad populations separated by a given
1053
1054 402 distance along the shore.

1055
1056
1057
1058 403
1059
1060
1061
1062
1063
1064

1065
1066
1067
1068
1069 404 **Acknowledgements**

1071 405 We thank the Canadian Wildlife Service and Ontario Parks for permission to study toads
1072
1073
1074 406 at Long Point and J. Middleton, E. Dirse, R. Card, S. Bosco Y.-T. Huang, S. Price, A. Merck, J.
1075
1076 407 Krohner, M. Warren-Paquin and G. Thomas, for field assistance. This research was funded by
1077
1078 408 grants from NSERC Canada, World Wildlife Fund Canada, Ontario Ministry of Natural
1079
1080 409 Resources and Forestry, Wildlife Preservation Canada, and the Canadian Wildlife Federation. P.
1081
1082 410 Marchand received support from the National Socio-Environmental Synthesis Center (SESYNC)
1083
1084 411 under funding received from the National Science Foundation (NSF) [grant number DBI-
1085
1086 412 1052875].
1087

1088 413
1089
1090 414 **Literature Cited**

- 1091
1092 415 Bartelt, P.E. and Peterson, C.R. 2000. A description and evaluation of a plastic belt for attaching
1093
1094 416 radio transmitters to western toads (*Bufo boreas*). – *Northwest. Nat.* **81**: 121–128.
1095
1096 417 Beaumont, M.A., Zhang, W. and Balding, D.J. 2002. Approximate Bayesian computation in
1097
1098 418 population genetics. – *Genetics* **162**: 2025–2035.
1099
1100 419 Beaumont, M. A. 2008. Joint determination of topology, divergence time, and immigration in
1101
1102 420 population trees. – In: Matsumura, S., Forster, P. and Renfrew, C. (eds.) *Simulation,*
1103
1104 421 *genetics, and human prehistory.* McDonald Institute for Archaeological Research,
1105
1106 422 Cambridge.
1107
1108 423 Benhamou, S. 2007. How many animals really do the Lévy walk? – *Ecology* **88**: 1962–1969.
1109
1110 424 Boenke, M. 2011. Terrestrial habitat and ecology of Fowler’s toads (*Anaxyrus fowleri*). – M.Sc.
1111
1112 425 thesis, Department of Biology, McGill University, Montreal, Canada.
1113
1114
1115
1116
1117
1118
1119
1120

1121
1122
1123
1124
1125
1126
1127
1128
1129
1130
1131
1132
1133
1134
1135
1136
1137
1138
1139
1140
1141
1142
1143
1144
1145
1146
1147
1148
1149
1150
1151
1152
1153
1154
1155
1156
1157
1158
1159
1160
1161
1162
1163
1164
1165
1166
1167
1168
1169
1170
1171
1172
1173
1174
1175
1176

- 426 Bradford, D.F. 2005. Factors implicated in amphibian population declines in the United States. –
427 In: Lannoo, M.J. (ed.), Amphibian declines: the conservation status of United States
428 species. Univ. of California Press.
- 429 Cecala, K.K., Price, S.J. and Dorcas, M.E. 2009. Evaluating existing movement hypotheses in
430 linear systems using larval stream salamanders. – *Can. J. Zool.* **87**: 292–298.
- 431 Chambers, J.M., Mallows, C.L. and Stuck, B.W. 1976. A method for simulating stable random
432 variables. – *J. Am. Stat. Assoc.* **71**: 340–344.
- 433 Clarke, R.D. (1974). Activity and movement patterns in a population of Fowler’s toad, *Bufo*
434 *woodhousei fowleri*. *American Midland Naturalist* **92**: 258-274.
- 435 COSEWIC (2010). COSEWIC assessment and status report on the Fowler’s Toad *Anaxyrus*
436 *fowleri* in Canada. – Committee on the Status of Endangered Wildlife in Canada. Ottawa.
437 vii + 58 pp. (www.sararegistry.gc.ca/status/status_e.cfm).
- 438 Csilléry, K., François, O. and Blum, M.G.B. 2012. abc: An R package for approximate Bayesian
439 computation (ABC). – *Methods Ecol. Evol.* **3**: 475–479.
- 440 Edwards, A.M. 2011. Overturning conclusions of Lévy flight movement patterns by fishing boats
441 and foraging animals. – *Ecology* **92**: 1247–1257.
- 442 Gautestad, A.O. and Mysterud, I. 2005. Intrinsic scaling complexity in animal dispersion and
443 abundance. – *Am. Nat.* **165**: 44–55.
- 444 Gautestad, A.O. and Mysterud, I. 2013. The Lévy flight foraging hypothesis: forgetting about
445 memory may lead to false verification of Brownian motion. – *Mov. Ecol.* **1**:9.

1177
1178
1179
1180
1181 446 Gelinas, P.J. and Quigley, R.M. 1973. The influence of geology on erosion rates along the north
1182 shore of Lake Erie. – In: Proc. Sixteenth Conf. Great Lakes Res., Int. Assoc. Great Lakes
1183 Res. 421–430.
1184 447
1185
1186 448
1187
1188 449 Gnedenko, B.V. and Kolmogorov, A.N. 1954. Limit distributions for sums of independent
1189 random variables. – Addison-Wesley.
1190 450
1191
1192 451 Gomez, J.M. and Zamora, R. 1999. Generalization vs. specialization in the pollination system of
1193 *Hormathophylla spinosa* (Cruciferae). – *Ecology* **80**: 796–805.
1194 452
1195
1196 453 Green, D.M. 2005. *Bufo fowleri*, Fowler’s toad. – In: Lannoo, M.J. (ed.), Amphibian declines:
1197 the conservation status of United States species. Univ. of California Press.
1198 454
1199
1200 455 Green, D. M., A. R. Yagi, and S. E. Hamill. 2011. Recovery Strategy for the Fowler’s Toad
1201 (*Anaxyrus fowleri*) in Ontario. – Ontario Recovery Strategy Series. Ontario Ministry of
1202 Natural Resources, Peterborough, Ontario. vi + 21 pp.
1203 456
1204
1205 457
1206
1207 458 Greenberg, D.A. and Green, D.M. 2013. Effects of an invasive plant on population dynamics in
1208 toads. – *Conserv. Biol.* **27**: 1049–1057.
1209 459
1210
1211 460 Hartig, F., Calabrese, J.M., Reineking, B., Wiegand, T. and Huth, A. 2011. Statistical inference
1212 for stochastic simulation models – theory and application – *Ecol. Letters* **14**: 816–827.
1213 461
1214
1215 462 Lowe, W.H. 2009. What drives long-distance dispersal? A test of theoretical predictions. *Ecology*
1216 **90**: 1456–1462.
1217 463
1218
1219
1220 464 Marchand, P., Harmon-Threatt, A.N. and Chapela, I. 2015. Testing models of bee foraging
1221 behavior through the analysis of pollen loads and floral density data. – *Ecol. Model.* **313**:
1222 41–49.
1223 465
1224 466
1225
1226
1227
1228
1229
1230
1231
1232

1233
1234
1235
1236
1237
1238
1239
1240
1241
1242
1243
1244
1245
1246
1247
1248
1249
1250
1251
1252
1253
1254
1255
1256
1257
1258
1259
1260
1261
1262
1263
1264
1265
1266
1267
1268
1269
1270
1271
1272
1273
1274
1275
1276
1277
1278
1279
1280
1281
1282
1283
1284
1285
1286
1287
1288

- 467 Marjoram, P., Molitor, J., Plagnol, V. and Tavaré, S. 2003. Markov chain Monte Carlo without
468 likelihoods. – *PNAS* **100**: 15324–15328.
- 469 Morales, J.M. 2002. Behavior at habitat boundaries can produce leptokurtic movement
470 distributions. – *Am. Nat.* **160**: 531–538.
- 471 Paradis, E., Braille, S.R., Sutherland, W.J. and Gregory, R.D. 1998. Patterns of natal and
472 breeding dispersal in birds. – *J. Anim. Ecol.* **67**: 518–536.
- 473 R Core Team. 2016. R: A language and environment for statistical computing. R Foundation for
474 Statistical Computing. Vienna, Austria. <http://www.R-project.org>.
- 475 Rowley, J.J.L. and Alford, R.A. 2007. Techniques for tracking amphibians: The effects of tag
476 attachment, and harmonic direction finding versus radio telemetry. – *Amphib.-Rept.* **2007**:
477 367–376.
- 478 Sisson, S.A., Fan, Y. and Tanaka, M.M. 2007. Sequential Monte Carlo without likelihoods. –
479 *PNAS* **104**: 1760–1765.
- 480 Skalski, G.T. and Gilliam, J.F. 2000. Modeling diffusive spread in a heterogeneous population: A
481 movement study with stream fish. – *Ecology* **81**:1685–1700.
- 482 Smith, M.A. and Green, D.M. 2005. Dispersal and the metapopulation paradigm in amphibian
483 ecology and conservation: are all amphibian populations metapopulations? – *Ecography*
484 **28**: 110–128.
- 485 Smith, M.A. and Green, D.M. 2006. Sex, isolation and fidelity: unbiased long-distance dispersal
486 in a terrestrial amphibian. – *Ecography* **29**: 649–658.

1289
1290
1291
1292
1293
1294
1295
1296
1297
1298
1299
1300
1301
1302
1303
1304
1305
1306
1307
1308
1309
1310
1311
1312
1313
1314
1315
1316
1317
1318
1319
1320
1321
1322
1323
1324
1325
1326
1327
1328
1329
1330
1331
1332
1333
1334
1335
1336
1337
1338
1339
1340
1341
1342
1343
1344

- 487 Stenson, R. 1993. The Long Point area: An abiotic perspective. – Long Point Environmental
488 Folio Series. Technical Paper #2. Heritage Resources Centre, University of Waterloo.
489 Waterloo, Ontario.
- 490 Storfer, A. 2003. Amphibian declines: future directions. – *Divers. Distrib.* **9**: 151–163.
- 491 Stuart, S.N., Chanson, J.S., Cox, N.A., Young, B.E., Rodrigues, A.S.L., Fischman, D.L. and
492 Waller, R.W. 2004. Status and trends of amphibian declines and extinctions worldwide.
493 *Science* **306**: 1783–1786.
- 494 Tavaré, S., Balding, D.J., Griffiths, R.C. and Donnelly, P. 1997. Inferring coalescence times from
495 DNA sequence data. – *Genetics* **145**: 505–518.
- 496 Toni, T., Welch, D., Strelkowa, N., Ipsen, A. and Stumpf, M.P.H. 2009. Approximate Bayesian
497 computation scheme for parameter inference and model selection in dynamical systems. –
498 *J. R. Soc. Interface* **6**: 187–202.
- 499 Uchaikin, V.V. and Zolotarev, V.M. 1999. Chance and stability: Stable distributions and their
500 applications. – De Gruyter, Utrecht.
- 501 Viswanathan, G.M., Buldyrev, S.V., Havlin, S., da Luz, M.G.E., Raposo, E.P. and Stanley, H.E.
502 1999. Optimizing the success of random searches. – *Nature* **401**: 911–914.
- 503 Wells 2007. The ecology and behavior of amphibians. – Univ. of Chicago Press.
- 504 Wikelski, M., Kays, R.W., Kasdin, N.J., Thorup, K., Smith, J.A. and Swenson, G.W. 2007.
505 Going wild: What a global small-animal tracking system could do for experimental
506 biologists. – *J. Exp. Biol.* **210**: 181–186.

1345
1346
1347
1348
1349
507 **Tables**
1350

	Model 1 predicted	Model 2 predicted	Model 3 predicted
Model 1 true	62.2%	3.2%	34.5%
Model 2 true	8.4%	88.4%	3.2%
Model 3 true	22.6%	3.0%	74.4%

1351
1352
1353
1354
1355
1356
1357
508

1359
509 Table 1: Confusion matrix for model selection, based on cross-validation results. For each model
1360
1361
510 version, we selected a random subset of 100 (out of 10,000) simulations, considered each
1362
1363
511 one in turn as the “data”, and applied the ABC model selection procedure (with a 5%
1364
1365
512 tolerance level) to determine which of the three model versions had the highest
1366
1367
513 probability of being the source of the simulated dataset.
1368
1369

1370
514

Parameter		α	γ (m)	p_0	d_0 (m)
Uniform prior range		(1, 2)	(10, 100)	(0, 1)	(20, 2000)
Model 1	Median	1.70	34	0.60	
	95% BCI	(1.41, 1.94)	(26, 42)	(0.53, 0.65)	
	CV error	10.3%	6.6%	1.0%	
Model 2	Median	1.83	46	0.65	
	95% BCI	(1.35, 1.99)	(34, 60)	(0.54, 0.72)	
	CV error	13.6%	7.6%	1.3%	
Model 3	Median	1.65	32	0.43	758
	95% BCI	(1.37, 1.91)	(26, 40)	(0.31, 0.59)	(220, 1697)
	CV error	10.0%	7.0%	4.8%	63.1%

1371
1372
1373
1374
1375
1376
1377
1378
1379
1380
1381
1382
1383
1384
1385
1386
1387
1388
515

1390
516 Table 2: Approximate Bayesian computation estimates of the simulation model parameters.

1391
1392
517 Posterior parameter distributions are obtained through selection of the 500 (out of
1393
1394
518 10,000) best-fitting parameter sets for each model version, followed by a local-linear
1395
1396
1397
1398
1399
1400

1401
1402
1403
1404
1405
1406
1407
1408
1409
1410
1411
1412
1413
1414
1415
1416
1417
1418
1419
1420
1421
1422
1423
1424
1425
1426
1427
1428
1429
1430
1431
1432
1433
1434
1435
1436
1437
1438
1439
1440
1441
1442
1443
1444
1445
1446
1447
1448
1449
1450
1451
1452
1453
1454
1455
1456

519 regression adjustment. The table shows the median and 95% Bayesian credible interval
520 (BCI) of the parameter's posterior distribution, along with the relative error estimated
521 from cross-validation (CV error).

522

1457
1458
1459
1460
1461
1462
1463
1464
1465
1466
1467
1468
1469
1470
1471
1472
1473
1474
1475
1476
1477
1478
1479
1480
1481
1482
1483
1484
1485
1486
1487
1488
1489
1490
1491
1492
1493
1494
1495
1496
1497
1498
1499
1500
1501
1502
1503
1504
1505
1506
1507
1508
1509
1510
1511
1512

523 **Figure captions**

524

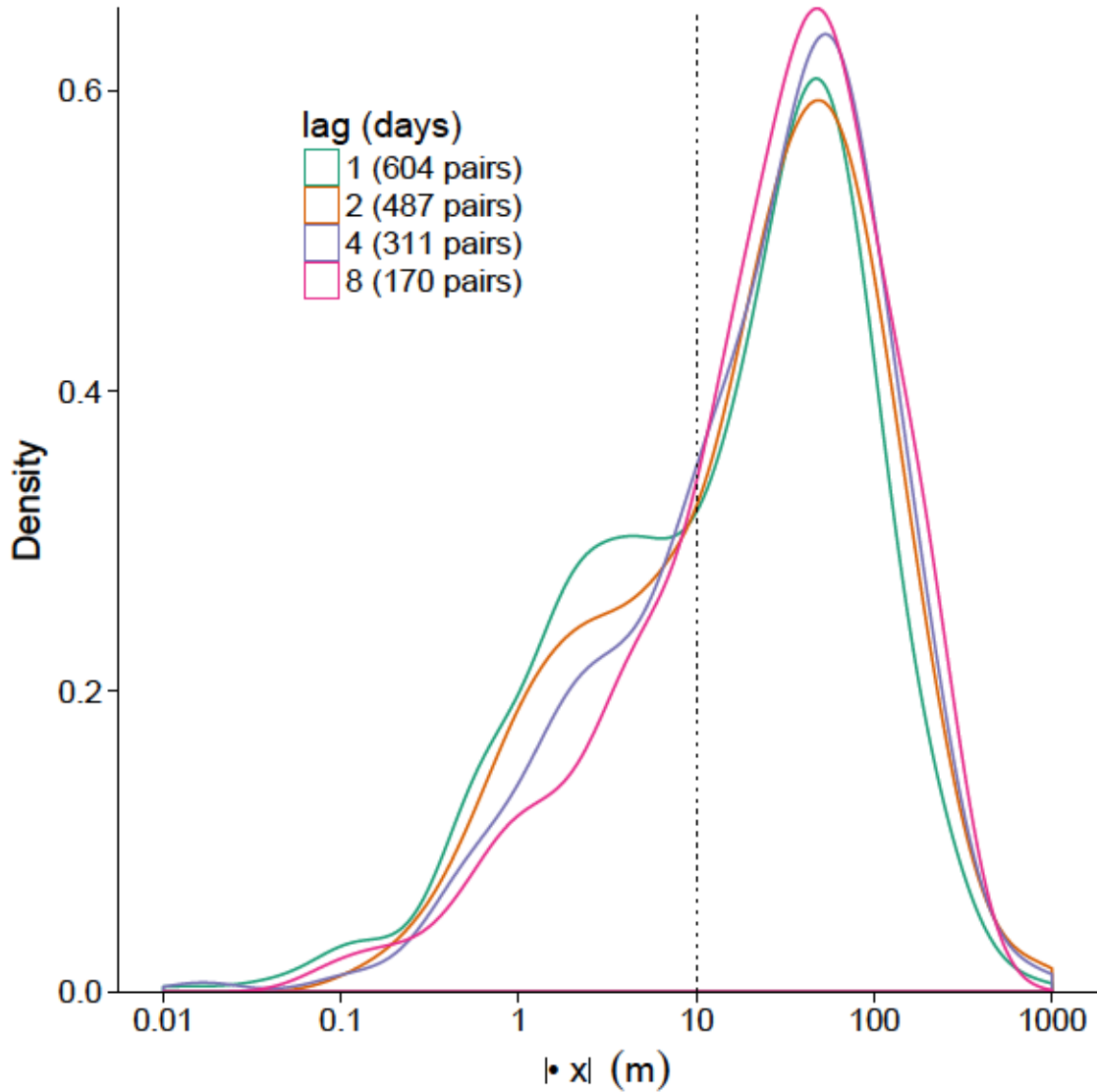
525 Figure 1: Kernel density estimates for the x -axis (parallel to shore) distance – shown here on a
526 log scale – between daytime refuges for time lags of 1, 2, 4 and 8 days. We calculated distances
527 between all pairs of fixes separated by the given time lag for each tracked toad. Distances
528 smaller than 10m (indicated by the finely dotted line) are within the GPS margin of error and
529 thus considered return events for the purpose of our model.

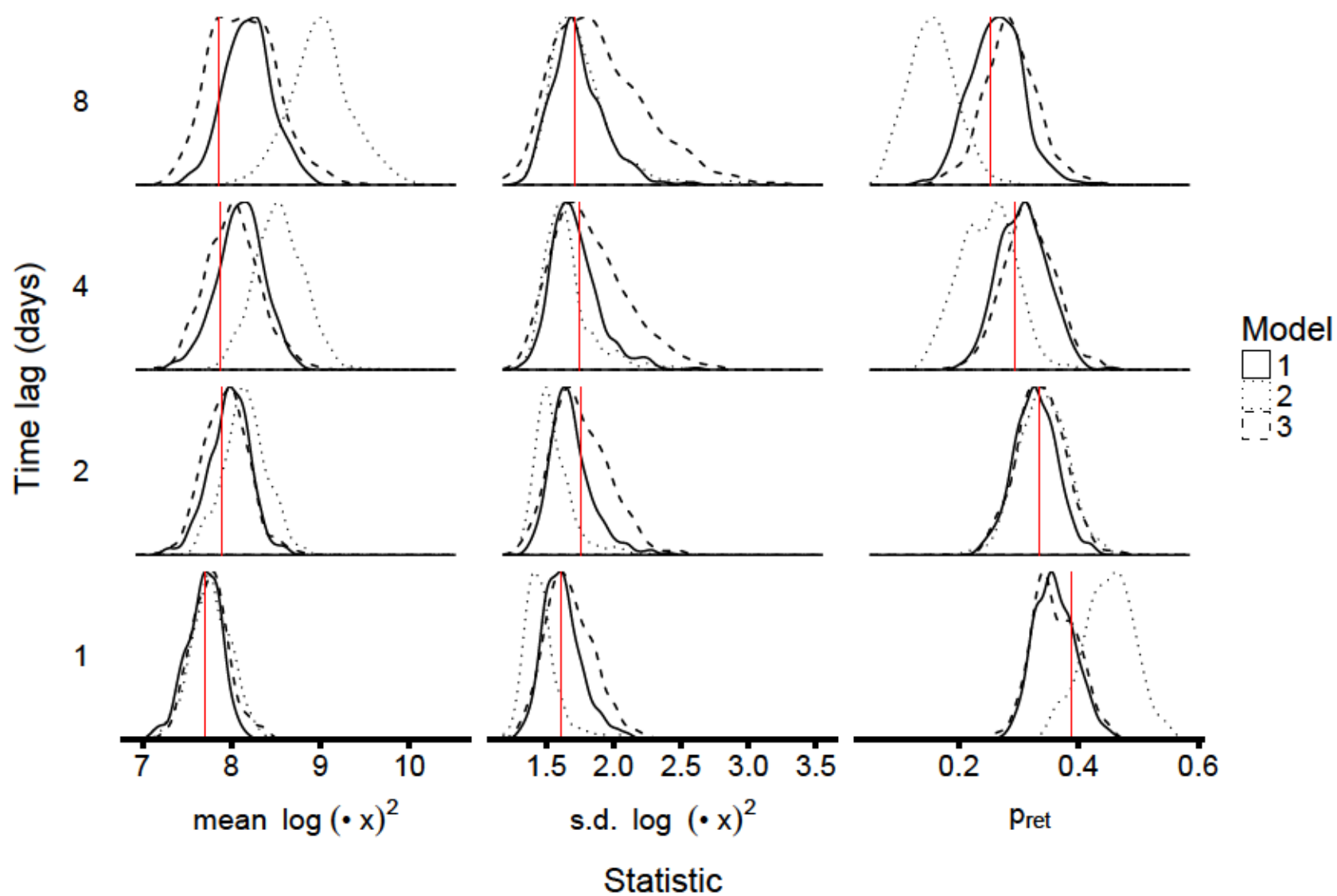
530

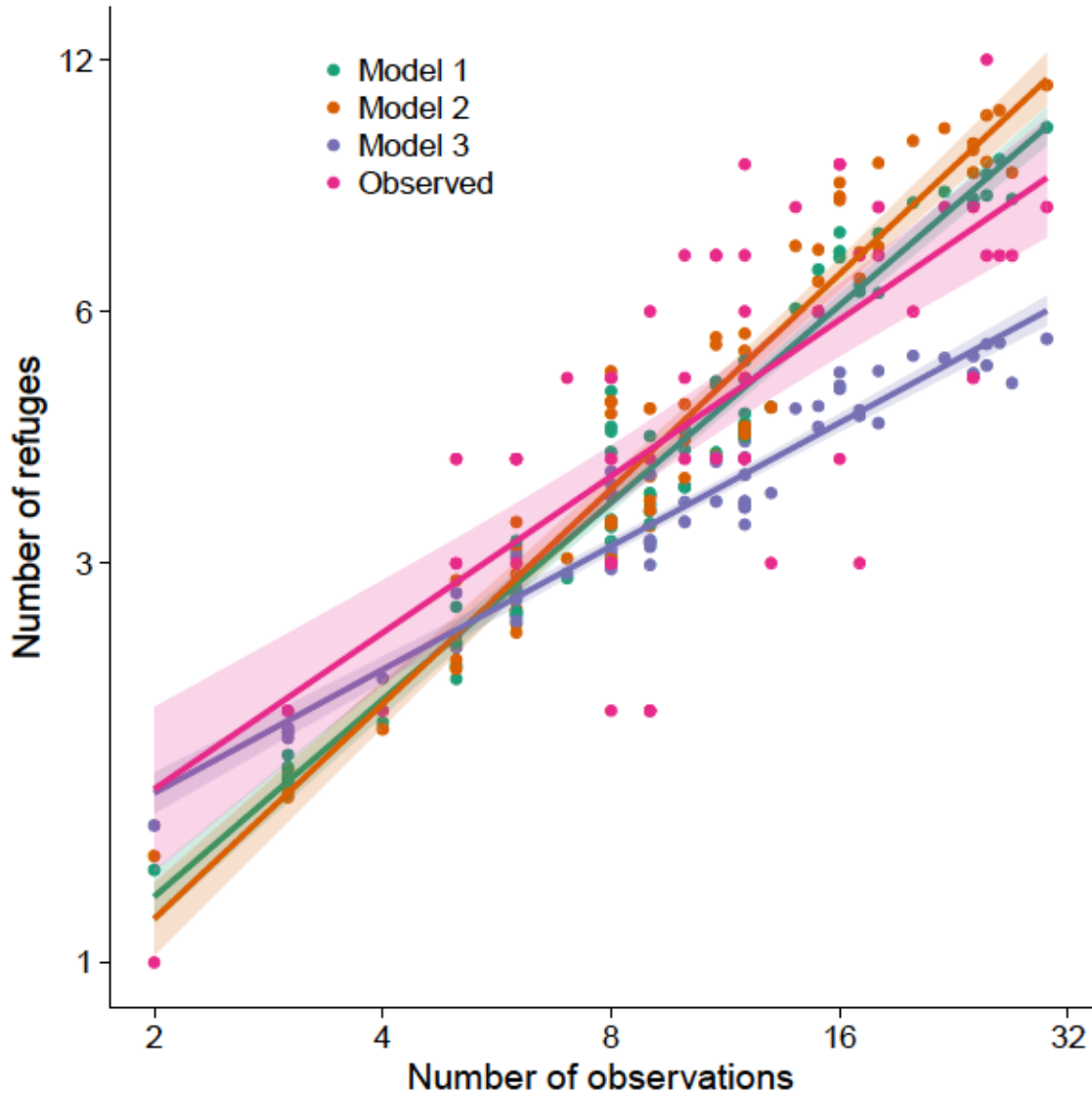
531 Figure 2: Kernel density estimates of the summary statistics from 500 simulations of each
532 movement model, with parameters drawn from the posterior distributions obtained by
533 approximate Bayesian computation. The red lines indicate the summary statistic's value in the
534 observed data.

535

536 Figure 3: Number of refuge sites (point clusters of diameter $< 10\text{m}$) as a function of the number
537 of radiotracking observations by toad for the three simulation model versions, compared with the
538 observed data. In each case, we estimate a linear trend on a log-log scale and show the
539 corresponding 95% confidence interval (shaded area). The simulated number of refuges shown
540 for each model version is the mean of 500 model runs with parameters drawn from their
541 posterior distribution.







A stochastic movement model reproduces patterns of site fidelity and long-distance dispersal in a population of Fowler's Toads (*Anaxyrus fowleri*)

Supplementary table

Tolerance	Model 1 estimation			Model 2 estimation			Model 3 estimation				Model selection		
	α	γ	ρ_0	α	γ	ρ_0	α	γ	ρ_0	d_0	Model 1	Model 2	Model 3
0.5%	16%	7.1%	1.3%	23%	6.9%	1.4%	17%	12.5%	6.4%	94%	37%	10%	31%
1%	13%	6.2%	1.0%	14%	7.4%	1.1%	12%	8.4%	4.7%	76%	36%	11%	28%
5%	10%	6.6%	1.0%	14%	7.6%	1.3%	10%	7.0%	4.8%	63%	38%	12%	26%
10%	11%	5.6%	1.2%	13%	7.0%	1.6%	10%	7.1%	5.0%	63%	39%	12%	27%

Table S1: Relative estimation and model selection errors calculated by cross-validation, as a function of the tolerance level (% of accepted simulations). The lowest value for each estimate is highlighted. For parameter estimation, the relative error is the mean square difference between the true parameter value and the estimated value, divided by the variance of the true parameter value across the 100 cross-validation replicates. The model selection error for model i is the fraction of cross-validation replicates of model i where the selected model was not i .

A stochastic movement model reproduces patterns of site fidelity and long-distance dispersal in a population of Fowler's Toads (*Anaxyrus fowleri*)

Supplementary figures

Fig. S1. Cross-validation results for the approximate Bayesian computation (ABC) estimation procedure, for (a) Model 1 (random return), (b) Model 2 (nearest return) and (c) Model 3 (distance-based return probability). For each model version, we selected a random sample of 100 (out of 10,000) simulation results, considered each one in turn as the “data” and ran the ABC-rejection algorithm (with 5% tolerance level) on the remainder of the simulation results to infer the true parameter values of the left out simulation. The diagonal line on each plot indicates equality between true and estimated values. The point estimates shown are the median of the posterior distribution, while error bars represent the 95% credible interval.

Fig. S2. Variation in the posterior parameter distribution quantiles (median and bounds of the 95% Bayesian credible interval) as a function of the number of simulations (N_{sim}), for (a) Model 1 (random return), (b) Model 2 (nearest return) and (c) Model 3 (distance-based return probability). The error bars show the 95% central range for each estimate and were obtained from 100 bootstrap replicates at each value of N_{sim} .

Figure S1(a)

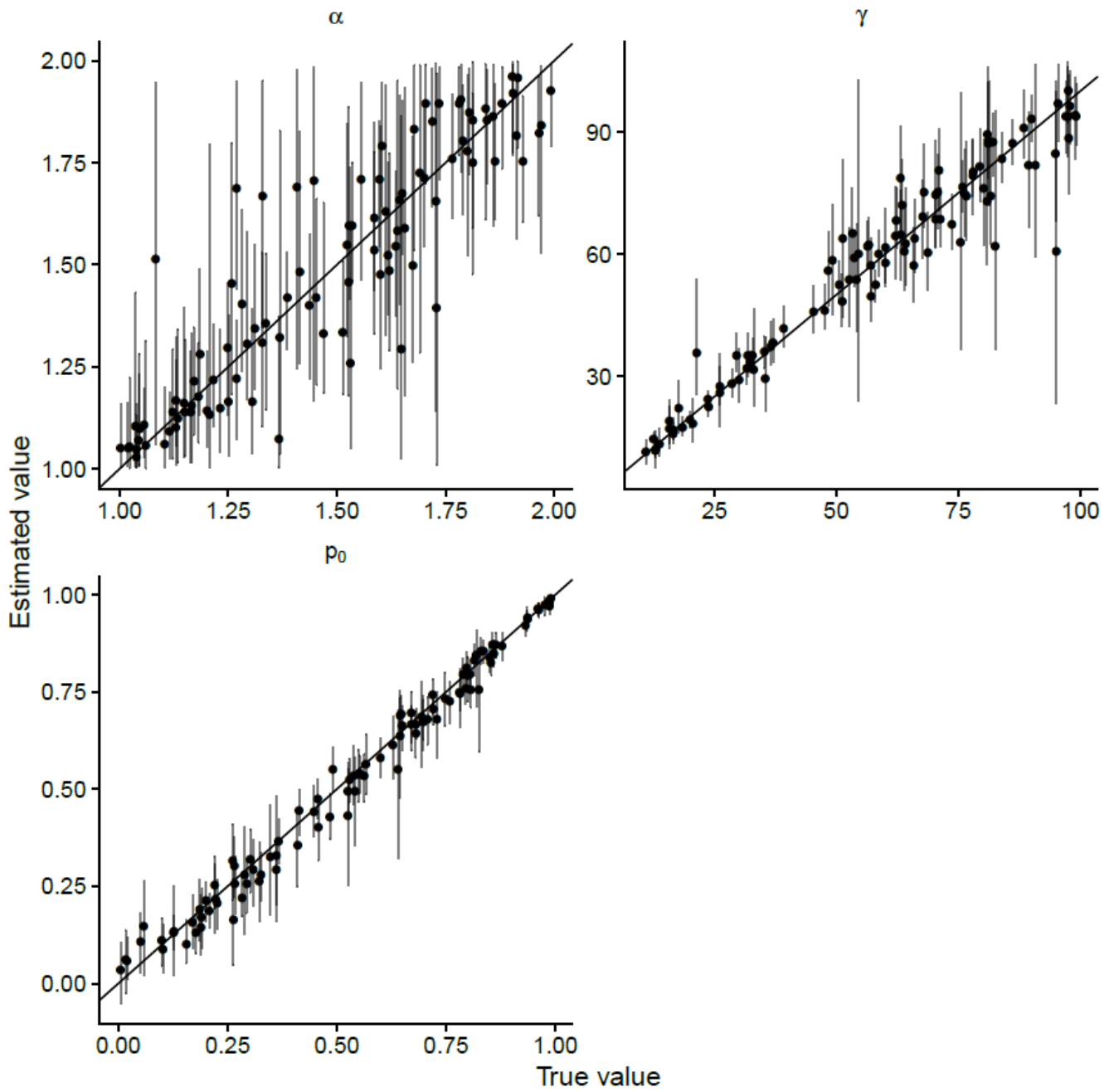


Figure S1(b)

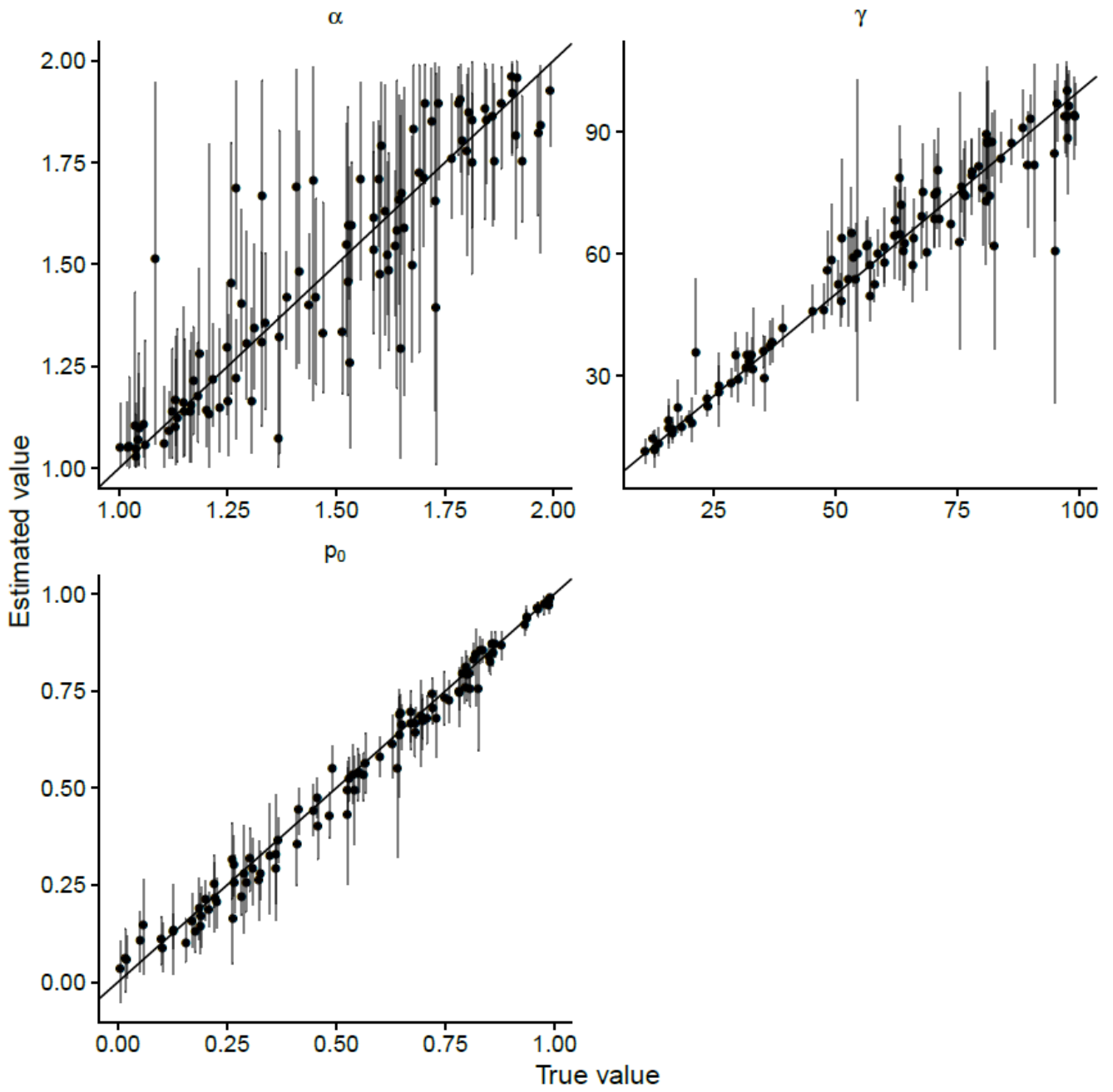


Figure S1(c)

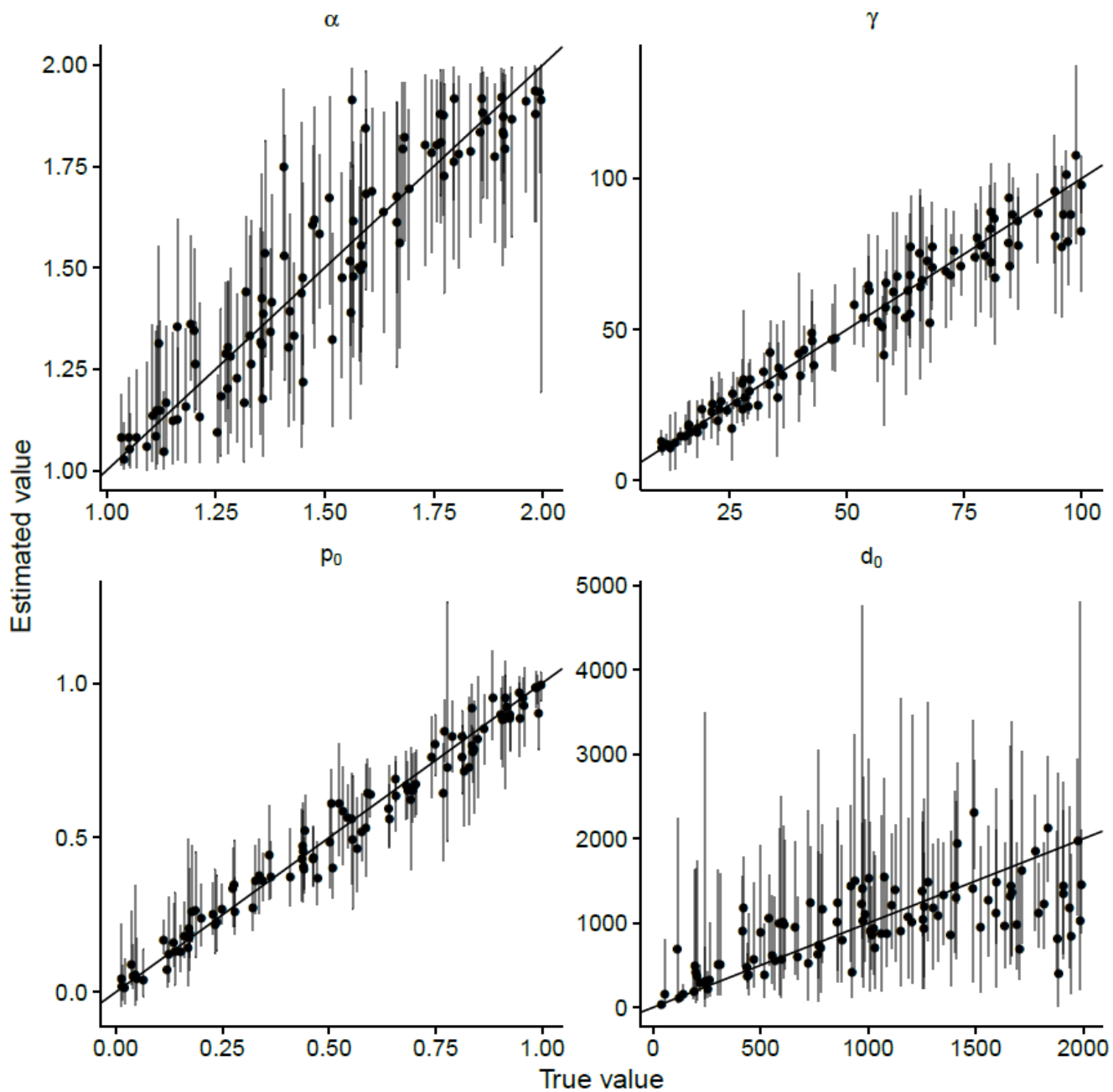


Figure S2(a)

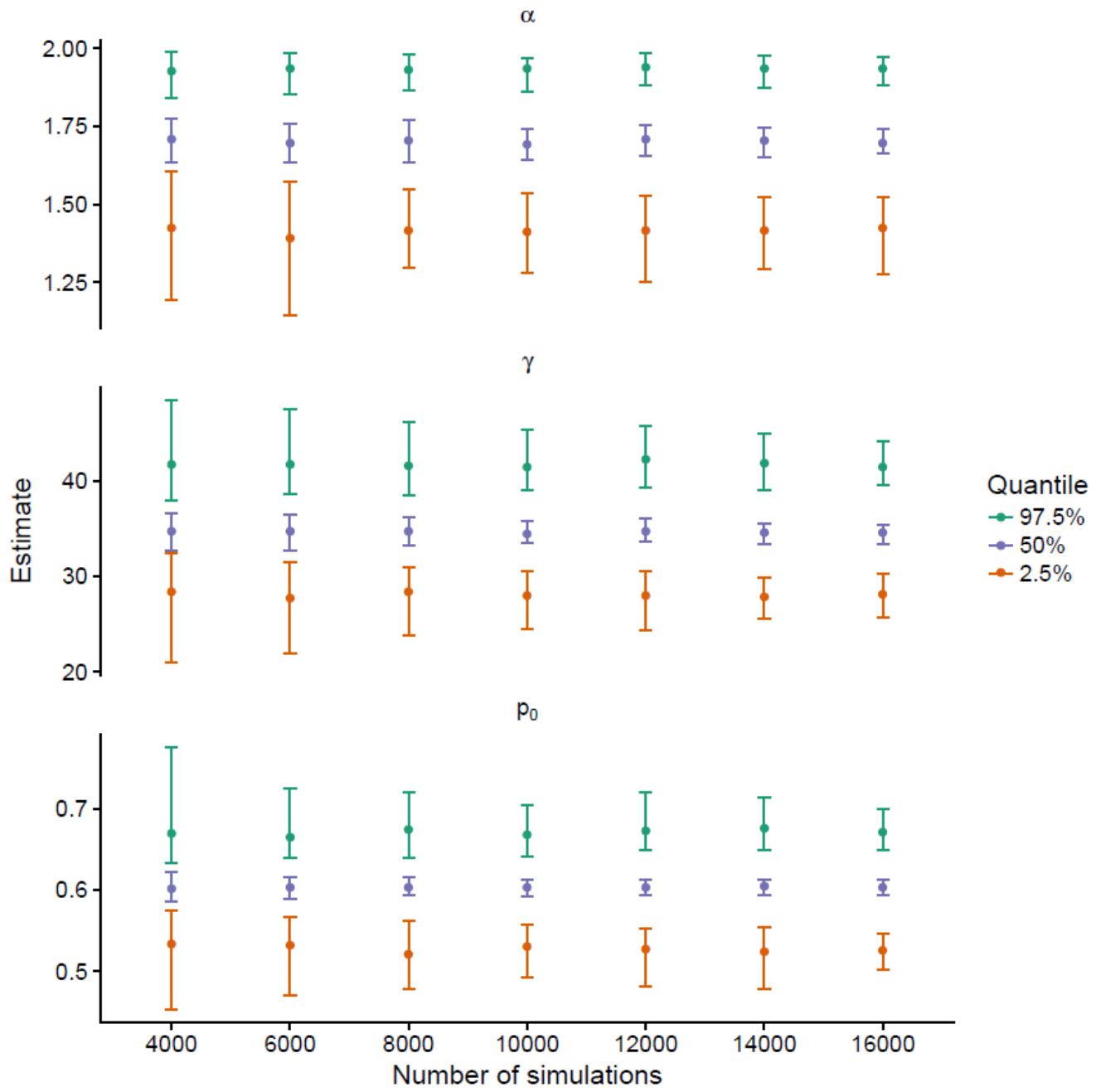


Figure S2(b)

